Bioorganic & Medicinal Chemistry 18 (2010) 4639–4647

Contents lists available at ScienceDirect

Bioorganic & Medicinal Chemistry

journal homepage: www.elsevier.com/locate/bmc

Globostelletins A–I, cytotoxic isomalabaricane derivatives from the marine sponge *Rhabdastrella globostellata*

Jin Li [a], Bo Xu [a], Jinrong Cui [a], Zhiwei Deng [b], Nicole J. de Voogd [c], Peter Proksch [d], Wenhan Lin [a,*]

[a] State Key Laboratory of Natural and Biomimetic Drugs, Peking University, Beijing 100083, People's Republic of China
[b] Analytical and Testing Center, Beijing Normal University, Beijing 100075, People's Republic of China
[c] National Museum of Natural History, PO Box 9517, 2300 RA Leiden, The Netherlands
[d] Institute of Pharmaceutical Biology and Biotechnology, Heinrich-Heine University, Düsseldorf D-40225, Germany

ARTICLE INFO

Article history:
Received 10 March 2010
Revised 9 May 2010
Accepted 11 May 2010
Available online 15 May 2010

Keywords:
Marine sponge
Rhabdastrella globostellata
Globostelletins A–I
Anti-tumor cells
Targeting ubiqitin-proteasome system
Structure–activity relationship

ABSTRACT

Nine new isomalabaricane-derived natural products, globostelletins A–I (**1**–**9**), were isolated from the marine sponge *Rhabdastrella globostellata*, together with jaspolides F (**10**), rhabdastrellic acid-A (**11**), (−)-stellettin E (**12**), stellettins C (**13**) and D (**14**). The structures of these compounds were determined on the basis of extensive spectroscopic analyses and by comparison with the reported data in the literature. The inhibitory activities of compounds **1**–**12** against human tumor cell lines were evaluated, and their structure–activity relationships were discussed. In addition, rhabdastrellic acid-A (**11**) showed potent inhibition against HL-60 cells, and it induced the apoptosis of HL-60 cells in M/G2 phase. The mechanism of **11** targeting the ubiquitin-proteasome system, including the regulation of ChT-L and T-L target proteins is discussed.

1. Introduction

Isomalabaricanes are a class of *trans-syn-trans* 6,6,5-tricyclic triterpenoids, which are found exclusively from marine sponges, mainly those of the genera *Stelletta*,[1–4] *Jaspis*,[5–9] *Geodia*,[10] and *Rhabdastrella*[11–17] (order Astrophorida). Their structures are characterized by the presence of a highly conjugated polyene system as a side chain to be positioned at C-13, while a ketone group is always located at C-12 of the tricyclic parent core. In addition, oxygenated functions are often present at C-3 of ring A and on the C-29 methyl group. The 13*Z* and 13*E* isomers are commonly found during isolation and purification. Numerous isomalabaricane-type triterpenoids have been found to have significant cytotoxic activity toward tumor cell lines.[18,19] The sponge *R. globostrella* is a rich source of isomalabraicane-type derivatives, which are considered to be the chemotaxonomic markers of the sponge genus *Rhabdastrella*. Thus far, more than 20 isomalabaricane-based metabolites have been reported from this sponge specimen. The structural patterns of this sponge vary markedly by ecological location.[12–16] For example, most of the isomalabaricanes from this species collected from coral reefs in Fiji showed oxygenated groups at C-22 and C-29, and displayed varying levels of inhibitory activity toward the A2780 ovarian cancer cell line due to stabilization of the binding of DNA with DNA polymerase β.[15] The same species growing in Mindanao in the Philippines produced a compound with a C-26 carboxylic group and the analogues terminated by an unsaturated δ-lactone.[11] Few reports have been discussed about the isomalabaricane terpenoids from the sponge *R. globostrella* distributed in the South China Sea, with the exception of rhabdastrellic acid-A.[17] Recently, we examined this sponge collected from Hainan Island in the South China Sea for the diverse minor metabolites, and here we report the isolation and characterization of 14 isomalabaricane-derived natural products, including nine new compounds.

2. Result and discussion

The MeOH extract of *Rhabdastrella globostellata* was partitioned between H_2O and CH_2Cl_2. A bioassay was used to assess the cytotoxicity of the fractions against human tumor cell lines including A549, BGC-823, HCT-8, Bel-7402, and A2780. The CH_2Cl_2 fraction showed inhibitory activity against A2780, whereas the H_2O fraction had weak cytotoxicity. The CH_2Cl_2 fraction was then subjected to vacuum liquid chromatography (VLC) using silica gel followed by the semi-preparative HPLC preparation to yield compounds **1**–**14**.

* Corresponding author. Tel.: +86 10 82806188; fax: +86 10 82802724.
E-mail address: whlin@bjmu.edu.cn (W. Lin).

0968-0896/$ - see front matter © 2010 Elsevier Ltd. All rights reserved.
doi:10.1016/j.bmc.2010.05.029

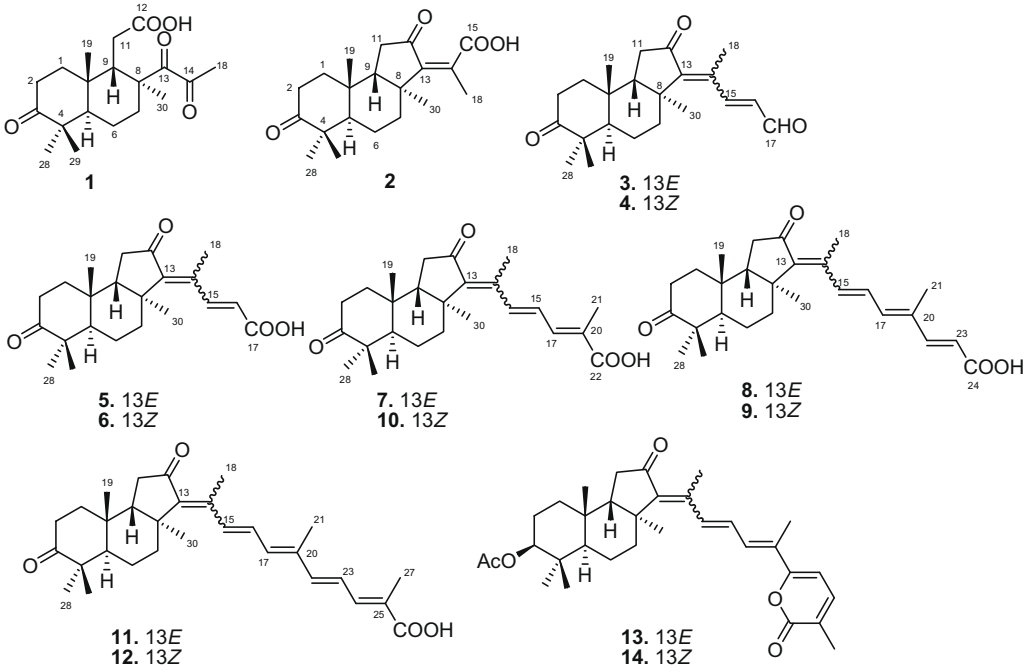

The molecular formula of globostelletin A (**1**) was determined to be $C_{19}H_{28}O_5$ by HRESIMS data (*m*/*z* 337.2010 $[M+H]^+$, calcd 337.2026). The IR spectrum showed absorption peaks at 1781 and 1707 cm^{-1}, indicating the presence of carbonyl groups, while the UV band at 244 nm indicated the absence of a conjugated polyene system, as seen for the side chain of other isomalabaricane triterpenoids. The ^{13}C NMR spectrum exhibited 19 resonances, including four carbonyl groups at δ_C 215.8 (C-3), 203.3 (C-13), 197.8 (C-14), and 178.8 (C-12); five methyls, five methylenes, two methines, and three alkyl quaternary carbons. The COSY and HMBC spectroscopic analysis led to the assignment of a drimane-type skeleton, in which a ketone was located at C-3, as evident from the methyl protons at δ_H 1.08 (s, CH_3-28) and 0.97 (s, CH_3-29) showing HMBC correlations with C-3, C-4 (δ_C 47.5), and C-5 (δ_C 46.3). An acetic acid moiety linked to C-9 was deduced from the COSY correlation between H_2-11 (δ_H 2.50, 2.52) and H-9 (δ_H 3.17). This assignment was supported by the HMBC interactions from H_2-11 to C-10 (δ_C 38.2), C-9 (δ_C 47.5), C-8 (δ_C 48.7), and C-12. In addition, the HMBC correlations of the methyl protons at δ_H 2.42 (CH_3-18) to the ketone carbons C-13 and C-14, together with the correlations of the methyl protons at δ_H 1.21 (CH_3-30) to C-8, C-9, and C-13, revealed a propandione group to be linked to C-8. Thus, the structure of **1** is assumed to be a derivative produced by oxidative cleavage at C-12 and C-15 of an isomalabaricane. The relative stereochemistry of **1** was assigned by NOESY spectrum. A *trans* fusion of the dicyclic nucleus was determined on the basis of the NOE interactions. The NOE correlations between CH_3-19/CH_3-29, CH_3-28/H-5 (δ_H 1.45), H-5/CH_2-11, CH_3-19/H-9, and CH_3-30/H_2-11 (Fig. 1) led the assignments of CH_3-19 β and H-9 β, whereas H-5, CH_2-11, and CH_3-30 were α-oriented.

Globostelletin B (**2**) had a molecular formula of $C_{20}H_{28}O_4$, as established by HRESIMS (*m*/*z* 687.3867 $[2M+Na]^+$, calcd 687.3873) and NMR data. The ^1H NMR spectrum (Table 1) showed an olefinic methyl resonance at δ_H 2.06 (s, CH_3-18), and four aliphatic methyl singlets at δ_H 0.85 (s, CH_3-19), 1.12 (s, CH_3-28), 1.05 (s, CH_3-29), and 1.38 (s, CH_3-30). The ^{13}C NMR and DEPT spectra displayed 20 carbon resonances, including two vinyl carbons at δ_C 144.9 (s, C-13) and 136.5 (s, C-14), and three carbonyl carbons at δ_C 219.1 (C-3), 204.3 (C-12), and 174.4 (C-15). The NMR spectroscopic data of **2** (Tables 1 and 2) were closely related to those of jaspolide D,[8] except for the presence of a carboxylic carbon C-15 in **2** instead of an aldehyde group of the latter compound. This assignment was confirmed by the HMBC correlations of CH_3-18 to olefinic carbons C-13, C-14, and C-15. The tricycle core was determined to be a *trans-syn-trans* geometry based on NOE interactions between CH_3-19/H-9 (δ_H 1.92, dd), CH_3-30/H-5 (δ_H 2.41, dd), and H-5/CH_3-28. The NOE cross-peak between CH_3-30/CH_3-18 was in agreement with 13*Z* configuration.

Globostelletins C and D (**3**–**4**) were a pair of inseparable geometrical isomers with a ratio of 1:1. The ESIMS spectrum showed a pseudomolecular ion peak at *m*/*z* 365 $[M+Na]^+$. The molecular formula of $C_{22}H_{30}O_3$ was determined from HRESIMS (*m*/*z* 365.2087 $[M+Na]^+$, calcd 365.2095), indicating eight degrees of unsaturation. The ^1H and ^{13}C NMR spectra of **3** and **4** were partially duplicated with regard to the 6,6,5-tricyclic nucleus, which was corresponded to that of **2**. The remaining NMR resonances were attributed to the C-13 bonded side chain which consisted of five carbons, including three olefinic carbons, a methyl group, and an aldehyde group. HMBC correlations determined that the side chain of **3** was identical to that of jaspiferal F.[7] The $J_{H\text{-}15/H\text{-}16}$ value (16.0 Hz) of **3** and **4** was indicative of a 15*E* configuration. The chemical shifts of CH_3-18 (δ_H 2.33) and H-15 (δ_H 7.60) in **3** were assigned to 13*E* as in the case of jaspiferal F. The NOE relationship between CH_3-30 (δ_H 1.45) and H-15 further confirmed this assignment. The 2D NMR correlations indicated the side chain

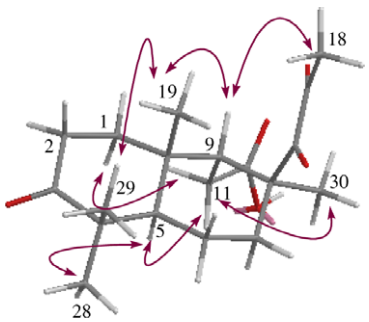

Figure 1. Key NOE correlations of **1**.

Table 1
^{1}H NMR (500 MHz) data (δ in ppm, J in Hz) of globostelletins A–I (**1**–**9**)[a]

No	1	2	3	4	5	6	7	8	9
1	1.80, ddd (6.5, 4.5, 13.0)	2.16, dd (9.8, 12.0)	2.18, dd (3.6, 14.4)	2.18, dd (3.6, 14.4)	2.17, dd (3.7, 14.2)	2.17, dd (4.8, 15.1)	2.20, dd (6.8, 12.5)	2.20, dd (2.7, 10.6)	2.20, dd (7.6, 14.7)
	1.57, ddd (4.0, 10.0, 13.0)	1.52, ddd (6.1, 9.3, 13.9)	1.57, m	1.57, m	1.55, ddd (6.1, 11.0, 14.2)	1.53, ddd (3.7, 9.5, 15.1)	1.57, ddd (6.3, 11.0, 12.5)	2.12, m	2.12, ddd (4.6, 11.0, 12.8)
2	2.66, ddd (6.5, 10.0, 15.5)	2.74, m	2.76, ddd (4.5, 4.0, 14.0)	2.76, ddd (4.5, 4.0, 14.0)	2.78, ddd (3.7, 11.0, 15.0)	2.75, ddd (4.8, 9.5, 15.0)	2.79, ddd (6.8, 11.0, 16.0)	2.76, ddd (2.7, 11.0, 15.5)	2.81, dd (7.6, 15.0)
	2.35, ddd (4.0, 4.5, 15.5)	2.38, dd (10.0, 13.4)	2.42, dd (12.5, 14.0)	2.42, dd (12.5, 14.0)	2.42, dd (6.1, 15.0)	2.43, dd (3.7, 15.0)	2.45, dd (6.3, 16.0)	2.49, ddd (8.0, 8.4, 15.5)	2.45, ddd (4.6, 11.0, 15.0)
5	1.45, dd (3.0, 12.5)	2.41, dd (2.0, 12.2)	2.42, dd (3.0, 14.4)	2.42, dd (3.0, 14.4)	2.42, dd (6.1, 14.0)	2.41, dd (6.8, 12.9)	2.42, dd (9.8, 3.2)	2.42, dd (8.8, 13.4)	2.42, dd (4.6, 11.0)
6	1.50, m	1.51, m	1.67, m	1.67, m	1.62, m	1.65, m	1.65, m	1.55, m	1.55, m
	1.61, m	1.62, m	1.55, m	1.55, m	1.55, m	1.55, m	1.55, m	1.67, m	1.66, m
7	2.28, ddd (4.0, 4.0, 14.0)	1.52, dd (5.4, 10.5)	2.20, dd (7.4, 14.4)	2.20, dd (7.4, 14.4)	2.27, dd (5.1, 12.6)	2.11, dd (7.6, 13.2)	2.26, dd (8.3, 14.2)	2.24, dd (10.6, 12.7)	2.24, dd (11.0, 13.5)
	1.13, ddd (4.0, 13.5, 14.0)	2.05, m	2.29, dd (4.4, 14.4)	2.29, dd (4.4, 14.4)	2.34, m	2.22, dd (4.6, 13.2)	2.20, dd (6.8, 12.5)	2.28, dd (9.5, 12.7)	2.28, dd (11.0, 13.5)
9	3.17, dd (2.0, 2.0)	1.92, dd (4.0, 8.0)	1.95, dd (5.1, 9.0)	1.95, dd (5.1, 9.0)	1.92, dd (5.8, 13.0)	1.91, dd (8.0, 15.0)	1.91, dd (7.0, 12.0)	1.90, dd (10, 12.5)	1.90, dd (10, 12.5)
11	2.52, dd (2.0, 15.0)	2.20, dd (4.0, 16.0)	2.28, dd (5.1, 13.5)	2.28, dd (5.1, 13.5)	2.32, dd (13.0, 13.5)	2.34, dd (15.0, 16.5)	2.29, dd (7.0, 16.0)	2.23, dd (10.0, 16.0)	2.23, dd (10.0, 16.0)
	2.50, dd (2.0, 15.0)	2.24, dd (8.0, 16.0)	2.30, dd (9.0, 13.5)	2.30, dd (9.0, 13.5)	2.28, dd (5.8, 13.5)	2.29, dd (8.0, 16.5)	2.26, dd (12.0, 16.0)	2.27, dd (12.5, 16.0)	2.27, dd (12.5, 16.0)
15			7.60, d (16.0)	8.86, d (16.0)	7.86, d (15.5)	8.96, d (16.0)	6.96, d (15.5)	6.86, d (15.0)	8.24, d (15.0)
16			6.56, dd (7.0, 16.0)	6.43, dd (7.0, 16.0)	6.28, d (15.5)	6.19, d (16.0)	6.99, dd (10.0, 15.5)	7.06, dd (11.5, 15.0)	6.96, dd (11.5, 15.0)
17			9.75, d (7.0)	9.73, d (7.0)			7.45, d (10.0)	6.62, d (11.5)	6.66, d (11.5)
18	2.42, s	2.06, s	2.33, s	2.08, s	2.31, s	2.05, s	2.37, s	2.37, s	2.10, s
19	0.99, s	0.85, s	0.90, s	0.90, s	0.89, s	0.89, s	0.89, s	0.88, s	0.88, s
21							2.08, s	2.03, s	1.99, s
22								7.50, d (15.5)	7.50, d (15.5)
23								6.02, d (15.5)	5.96, d (15.5)
28	1.08, s	1.12, s	1.14, s	1.15, s	1.14, s	1.14, s	1.08, s	1.15, s	1.15, s
29	0.97, s	1.05, s	1.09, s	1.09, s	1.07, s	1.08, s	1.15, s	1.08, s	1.08, s
30	1.21, s	1.38, s	1.45, s	1.50, s	1.47, s	1.42, s	1.47, s	1.46, s	1.43, s

[a] In $CDCl_3$.

Table 2
^{13}C NMR (125 MHz) data of globostelletins A–H (**1**–**8**)[a]

No.	1	2	3	4	5	6	7	8
1	35.3, t	31.2, t	31.3, t	31.3, t	31.3, t	31.3, t	31.3, t	31.3, t
2	34.7, t	33.3, t	33.3, t	33.3, t	33.3, t	33.3, t	33.4, t	33.4, t
3	215.8, s	219.1, s	219.5, s	219.5, s	218.8, s	218.7, s	218.9, s	219.0, s
4	47.5, s	46.8, s	46.8, s	46.8, s	46.8, s	46.8, s	46.8, s	46.8, s
5	46.3, d	45.3, d	45.4, d	45.4, d	45.4, d	45.4, d	45.4, d	45.4, d
6	20.0, t	19.1, t	19.7, t	19.5, t	19.6, t	19.5, t	19.7, t	19.5, t
7	31.1, t	35.3, t	36.6, t	36.6, t	38.5, t	36.7, t	38.6, t	38.5, t
8	48.7, s	40.1, s	38.7, s	38.7, s	45.3, s	44.9, s	45.0, s	45.0, s
9	47.5, d	48.2, d	47.5, s	47.6, s	47.5, d	47.7, d	47.7, d	47.8, d
10	38.2, s	34.8, s	34.8, s	34.8, s	34.8, s	34.8, s	34.8, s	34.8, s
11	31.3, t	34.8, t	38.7, t	38.7, t	36.5, t	36.4, t	36.6, t	36.6, t
12	178.8, s	204.3, s	206.8, s	206.8, s	207.1, s	205.6, s	207.1, s	206.0, s
13	203.3, s	144.9, s	152.2, s	152.2, s	151.7, s	151.0, s	148.5, s	147.6, s
14	197.8, s	136.5, s	138.0, s	138.0, s	137.9, s	138.5, s	140.4, s	141.0, s
15		174.4, s	150.5, d	150.7, d	145.5, d	145.2, d	139.4, d	136.8, d
16			133.7, d	132.1, d	123.4, d	121.8, d	130.1, d	131.0, d
17			193.1, d	194.9, d	170.4, s	170.5, s	139.7, d	139.2, d
18	26.4, q	16.9, q	14.5, q	15.9, q	14.3, q	15.9, q	14.4, q	14.5, q
19	21.8, q	23.4, q	23.5, q	23.5, q	23.4, q	23.4, q	23.4, q	23.4, q
20							128.8, s	136.3, s
21							12.8, q	12.8, q
22							172.0, s	150.2, d
23								117.1, d
24								171.0, s
28	25.5, q	29.2, q	29.2, q	29.0, q	29.2, q	29.2, q	29.2, q	29.2, q
29	21.5, q	19.3, q	19.3, q	19.3, q	19.3, q	19.3, q	19.3, q	19.3, q
30	26.3, q	24.6, q	24.2, q	26.4, q	26.3, q	24.3, q	26.0, q	26.0, q

[a] In $CDCl_3$.

composition of **4** to be identical to that of **3**. The differences were found by the upfield shifted CH_3-18 (δ_H 2.08) and the downfield shifted H-15 (δ_H 8.86) of **4** due to H-15 to be located in the deshielding region of the ketone group C-12, indicating **4** to be a 13*Z* isomer. This assignment was also confirmed by the NOE correlation observed between CH_3-18 and CH_3-30.

The molecular formula of globostelletin E (**5**) was determined to be $C_{22}H_{30}O_4$ by HRESIMS (*m*/*z* 359.2217 $[M+H]^+$, calcd 359.2224) and NMR data, indicating eight degrees of unsaturation. Comparison of its NMR data (Tables 1 and 2) with those of **3** revealed the only difference due to the presence of a carboxylic carbon (δ_C 170.4) at C-17, instead of the aldehyde group found in **3**. The chemical shifts of CH_3-18 (δ_H 2.31, s) and H-15 (δ_H 7.86) were in agreement with 13*E*. The coupling constant $J_{15,16}$ (15.5 Hz), together with NOE interactions between H_3-18/H-16 (δ_H 6.28, d), confirmed 15*E* geometry in the side chain.

The NMR spectroscopic data of globostelletin F (**6**) were closely related to those of **5**, and the 2D NMR data analysis revealed both compounds having the same gross structure. However, H-15 of **6** was shifted significantly to downfield at δ_H 8.96 (d, J = 16 Hz), whereas CH_3-18 was shifted to upfield at δ_H 2.05 in comparison with those of the corresponding protons of **5**. These findings indicated a 13*Z* configuration of **6**. The NOE correlations between CH_3-18/CH_3-30 and H-16 (δ_H 6.19)/CH_3-18, along with the $J_{H\text{-}15/H\text{-}16}$ value confirmed that **6** is a 13*Z* isomer of **5.**

Interpretation of 1D and 2D NMR spectroscopic data of globostelletin G (**7**) revealed that it is an 13*E* isomer of jaspolide F (**10**),[8] as evident from the significant upfield shift of H-15 (δ_H 6.96) and the downfield shifted H_3-18 (δ_H 2.37) compared with the corresponding signals of **10**.

The HRESIMS of globostelletin H (**8**) showed a pseudo molecular ion peak at *m*/*z* 447.2506 $[M+Na]^+$, which was in agreement with a molecular formula of $C_{27}H_{36}O_4$ with 10 degrees of unsaturation. The UV bands at 266 and 367 nm suggested the presence of a highly conjugated chromophore. ^{1}H NMR spectrum showed the resonances for six olefinic protons around δ_H 6.02–7.50 ppm, and six methyl singlets at δ_H 0.88, 1.15, 1.08, 1.46, 2.37, and 2.03. An olefinic ABX spin system at δ_H 6.86 (1H, d, J = 15.0 Hz, H-15), 7.06 (1H, dd, J = 11.5, 15.0 Hz, H-16), and 6.62 (1H, d, J = 11.5 Hz, H-17) and an AB spin system at δ_H 7.50 (1H, d, J = 15.5 Hz, H-22) and 6.02 (1H, d, J = 15.5 Hz, H-23) were attributed to the side chain.

Table 3
Inhibitory effects of **1–12** on tumor cell lines

Compounds	IC_{50} (μM)				
	HCT-8	Bel-7402	BGC-823	A549	A2780
1	>50	>50	>50	>50	>50
2	>50	>50	>50	>50	>50
3–4	22.03	31.24	28.77	>50	9.04
5	>50	>50	>50	>50	17.36
6	>50	>50	>50	>50	>50
7	>50	>50	>50	>50	15.37
8	>50	>50	>50	>50	8.19
9	>50	>50	>50	>50	7.66
10	>50	>50	>50	>50	7.92
11	>50	21.18	>50	>50	4.23
12	>50	13.70	>50	18.61	<0.5

The ^{13}C NMR spectrum revealed a total of 27 carbon resonances, that were assigned to eight olefinic carbons, a carboxylic acid (δ_C 171.0), and two ketones (δ_C 206.0, 219.0). The NMR data of **8** were characteristic of an isomalabaricane-type terpenoid, closely related to rhabdastrellic acid-A (**11**).[17] However, a carboxylic group of **8** was linked to C-23 instead of a methacrylic acid group found in **11**. The HMBC correlation of the typical downfield shifted H-22 (δ_H 7.50) with the carboxylic carbon at δ_C 171.0 (C-24) confirmed this assignment. The chemical shift of CH_3-18 (δ_H 2.37) indicated it to be deshielded by the C-12 carbonyl function. Thus, C-13 of **8** was assigned to *E*-configuration. The *E*-configurations of C-15, C-17, and C-22 were determined from the J values of H-15/H-16 (15.0 Hz), along with the NOE correlations between CH_3-30/H-15, H-15/H-17, H-17/H-22, H-23/CH_3-21, H-23/CH_3-27, CH_3-21/H-16, and H-16/CH_3-18.

Globostelletin I (**9**) had the same molecular formula as **8**, as determined by HRESIMS analysis (*m*/*z* 425.2686 $[M+H]^+$, calcd 425.2675). Comparisons of the ^{1}H NMR data revealed the similarity of both compounds, with the exception of the chemical shifts of

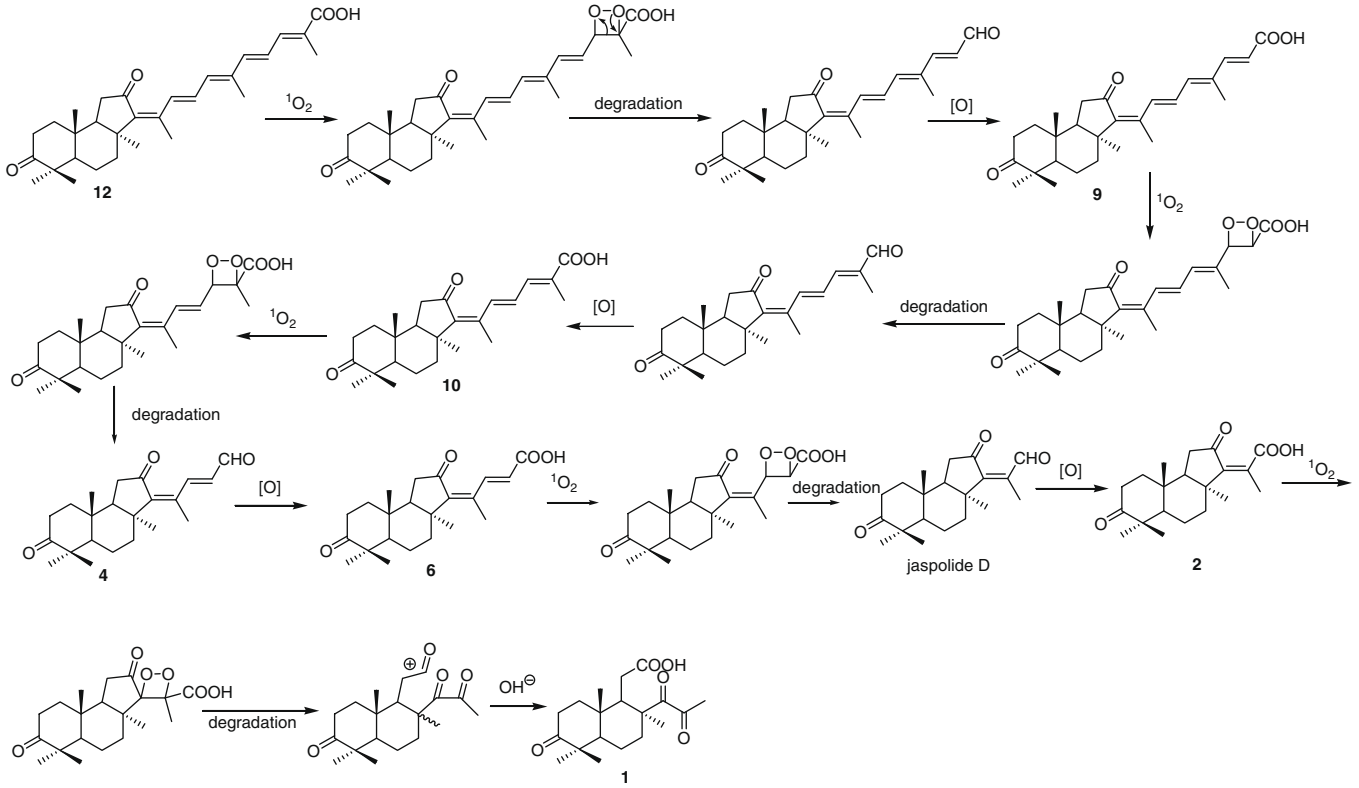

Figure 2. Postulated biogenetic degradation from **12** to **1**.

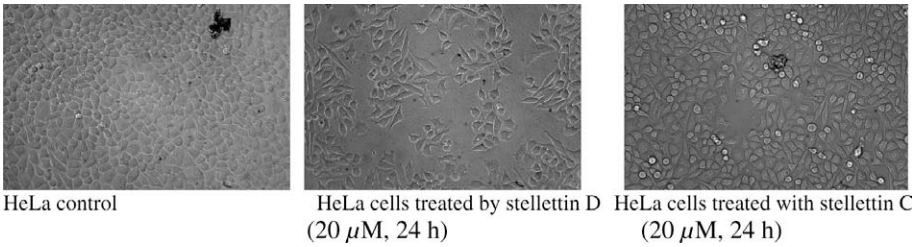

Figure 3. Morphological changes in HeLa cells after treatment with stellettins C and D.

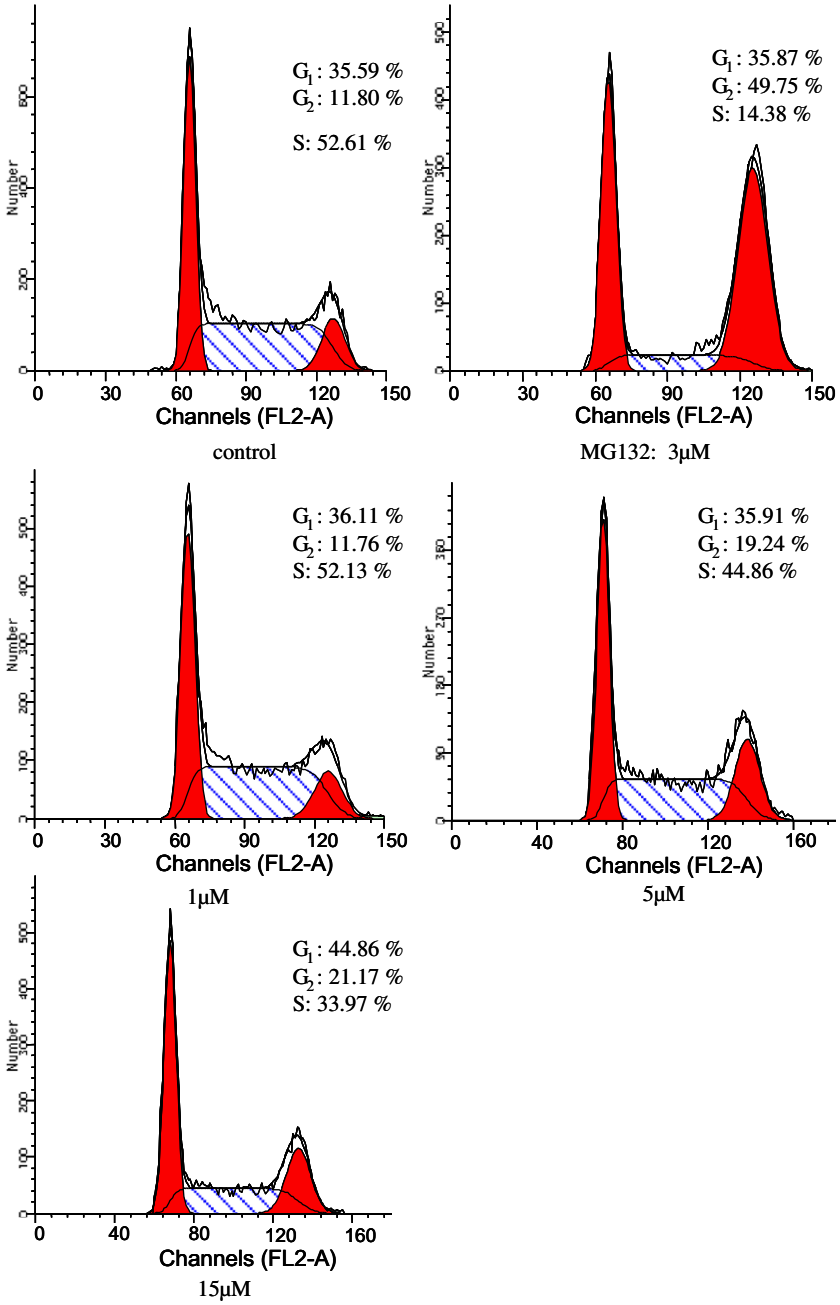

Figure 4. The effects **11** on HL-60 cell cycle with different doses.

H-15 and CH_3-18. The downfield shifted H-15 δ_H 8.24 (d, J = 15.0 Hz) was in contrast to CH_3-18, shifted relatively upfield, as seen in jaspolide F (**10**). These data indicated that **9** is a 13*Z* isomer of **8**.

Based on the spectroscopic analyses and comparison with the reported data in the literature, compounds **10**–**14** were determined as identical to jaspolide F,[8] rhabdastrellic acid-A,[7] (−)-stellettin E,[2] stellettins C and D,[2] respectively.

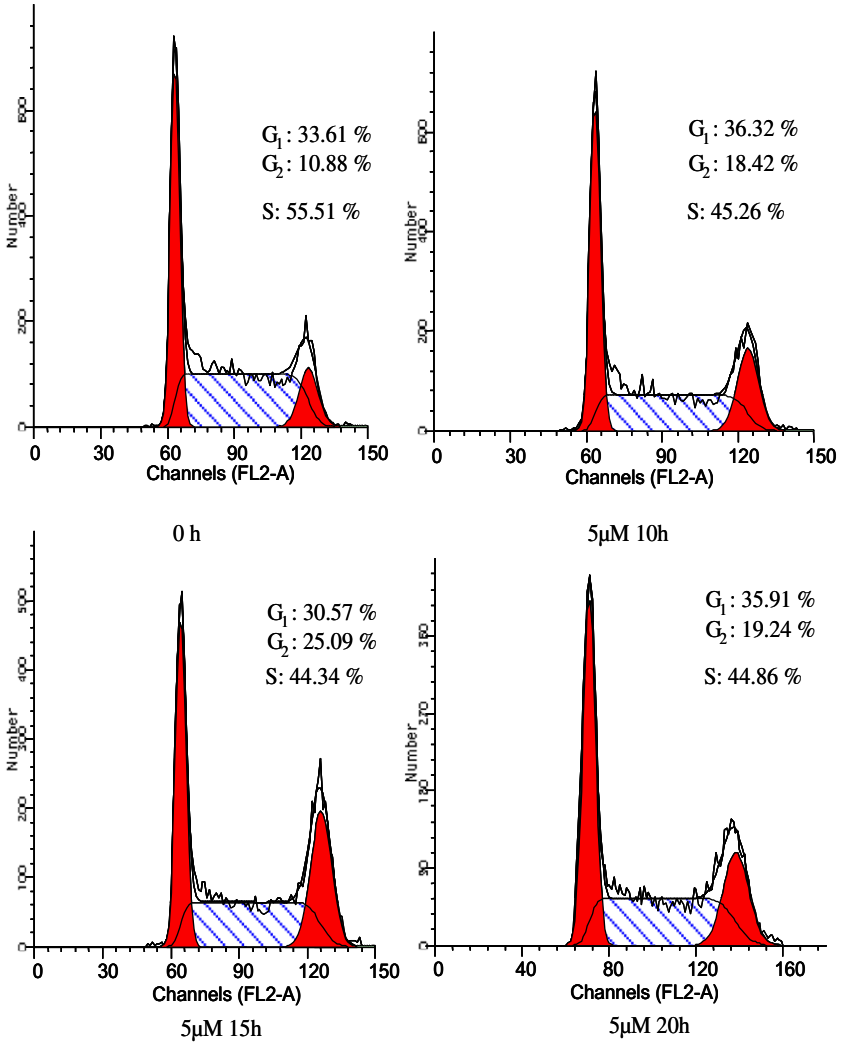

Figure 5. The effects of **11** on cell cycle with different times.

Isomalabaricatrienol as produced by Tyr510 mutants is considered a putative precursor of isomalabaricane triterpenoids in sponges.[20,21] Thus, the various lengths of the side chains of compounds **1**–**12** are assumed as the products to be generated by oxidative degradation from isomalabaricane triterpenoid[22] (Fig. 2). The isomerization between 13*Z* and 13*E* geometric isomers was suggested to be induced by light irradiation during a separation process.

Compounds **1**–**12** were tested against human tumor cell lines (A549, BGC-823, HCT-8, Bel-7402, and A2780). Most of them showed selectively inhibitory activities against human ovarian carcimona A2780 cell line (Table 3), and the effects varied due to the length of the side chain. Compounds **11** and **12,** with five conjugated double bonds, showed dramatically inhibitory activity toward A2780, and the inhibitory rate decreased markedly when the numbers of double bonds in side chain were reduced, as in the cases of **2**, **5**, and **6** which showed weakly inhibition. In addition, 13*Z*-isomalabaricanes (**12**, **9**–**10**) showed more inhibitory activity than 13*E* isomers (**11**, **7**–**8**), with the exception of the mixture of **3**–**4** which showed more effective inhibition. Additional example is due to the geometric isomers stellettins D and C, the former (13*Z* configuration) showed more inhibitory activities against HL-60 (IC_{50} = 0.01 μM) and HeLa cells (IC_{50} = 7.5 μM) compared to that of the latter (13*E*) (IC_{50} = 16 μM for HeLa and 3.6 μM for HL-60). The morphological changes in HeLa cells after treatment with stellettins C and D are showed in Figure 3. A comparison of the inhibitory activities of **3** and **4** with that of **5** and **6** revealed

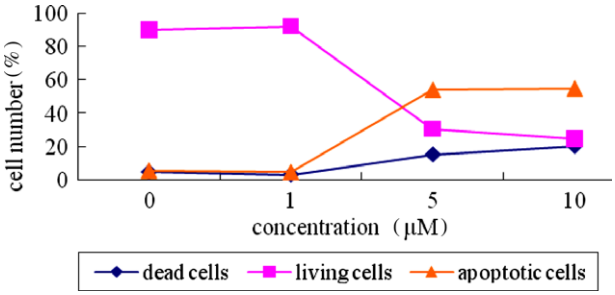

Figure 6. The effects of **11** on HL-60 cell apoptosis in different doses.

that the isomalabaricanes terminated by aldehyde group increased cytotoxicity in comparison with those terminated by a carboxyl group.

In addition, rhabdastrellic acid-A (**11**) effectively inhibited proliferation of the human promyelocytic leukemia cell line HL-60 (IC_{50} = 6.7 μM). In order to investigate the effect of **11** on cell cycle, HL-60 cells were treated with different doses of **11** for 20 h before subjected to cell cycle analysis. DNA histogram analysis indicated that **11** induced G2/M arrest of the cell cycle in dose-dependent manner and the percentage of cells in G2/M phase increased by 19.2% and 21.2% after adding 5.0 and 10 μM of **11**, respectively (Fig. 4). The effect of **11** (5 μM) on cell cycle was also in

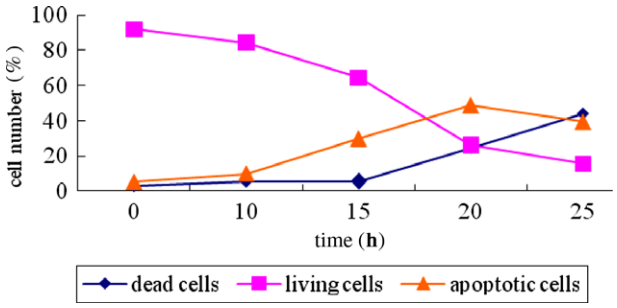

Figure 7. The effects of **11** on HL-60 cell apoptosis in different times.

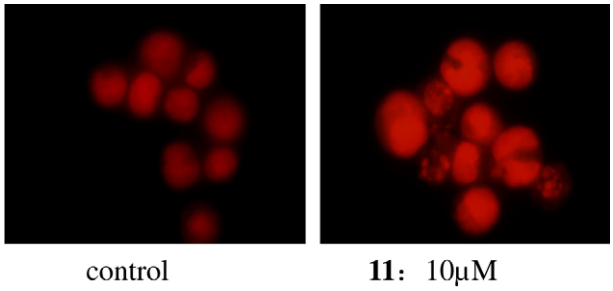

Figure 8. The morphological change of HL-60 cells induced by **11**.

time-dependent and the percentage of cells in G2/M phase increased from 10.9% to 18.4% and 25.1% at the checking-points 10 and 15 h, respectively (Fig. 5). The progressive G2/M accumulation as induced by **11** was largely associated with a concomitant decrease of cells.

The gene $p21^{WAF1/Cip1}$ plays important role in the cell cycle progression regulation, and over-express $p21^{WAF1/Cip1}$ could halt the cell arrest at G2 phase.[23] By western blot analysis, the expression of p21 in HL-60 cells was up-regulated gradiently followed by the increasing the doses of **11**. This result led to the consideration that compound **11** inducing G2/M arrest is related to the up-regulation of $p21^{WAF1/Cip1}$.

To assess whether rhabdastrellic acid-A (**11**) induced apoptosis, the multiparameter flow cytometry (annexin V-FITC/PI) was used to monitor the early stages of apoptosis. In these stages, the cell damage results in the changes of the phospholipids content of the plasma membrane outer leaflet, and phosphatidylserine is exposed at the external surface of the cells. Annexin V is a Ca^{2+}-dependent phospholipids-binding protein with high affinity for phosphatidylserine. In addition, this method is also able to discriminate the living cells, early apoptotic cells (pro-apoptotic cells), and dead cells (late apoptotic and necrotic cells). As showed in Figure 6, the increasing apoptotic HL-60 cells were correlated to the doses of **11**. The pro-apoptotic cells increased significantly from original 5.53% (control) to 53.92% after treatment with **11** (5 μM). However, the dead cells increased slowly from 15.34% to 20.46% after treatment with the same dose. This fact indicated that a pathway to inhibit the HL-60 proliferation by **11** is related to cell apoptosis. Treated with **11** (5 μM), the pro-apoptotic HL-60 cells increased linearly from 5.16% to 9.93%, 29.76%, and 48.84%, respectively, at the checking-points of 0 h, 10 h, 15 h, and 20 h, indicating the pro-apoptosis is also time-depended. Accordingly, the dead cells increased from 24.45% (20 h) to 43.96% (25 h) (Fig. 7).

The morphological changes of HL-60 cells provided additional information about the cell apoptosis induced by compound **11**. After incubation with **11** (10 μM) for 10 h, HL-60 cells exhibited membrane blebbing, cellular shrinkage, chromatin condensation, and fragmentation. The typical apoptotic cell bodies were visualized by using fluorescent microscopy (Fig. 8).

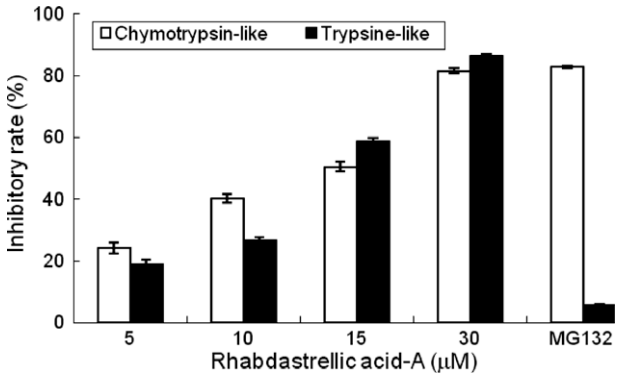

Figure 9. The inhibitory effects of **11** on ChT-L and T-L of 20S proteasome by different doses in 5 h.

Ubiquitin-proteasome (UPP) system is responsible for the degradation of most intracellular proteins, including those to control cell cycle progression, apoptosis, signal transduction and the NF-κB transcriptional pathway, such as p53, c-Myc, $p21^{WAF1/Cip1}$, IκB, and cyclines.[24] Aberrations in the ubiquitin-proteasome system underlie the pathogenesis of many human diseases. Thus, both the ubiquitin-conjugating system and the 20S proteasome are important targets for drug discovery. Eukaryotic 20S proteasome presents three major activities, namely chymotrypsine-like (ChT-L), trypsine-like (T-L) and peptidyl-glutamy-peptide hydrolysing (PGPH) activities. Proteasome inhibitors such as MG132 showed potent effects to inhibit several kind of cancer cells,[25–27] and these results prompted us to examine whether compound **11** inducing apoptosis in tumor cells related to the UPP signaling pathway. We checked the direct effect of **11** on proteasome ChT-L and T-L activities. Proteasome purified from human erythrocytes was incubated for 1 h with **11** by various doses in the presence of the specific fluorogenic substrate for the detection of ChT-L and T-L peptide cleavage. The experimental results indicated that **11** (30 μM) significantly inhibited ChT-L and T-L sites with the rates of 81.5% and 86.3%, respectively (Fig 9), whereas MG132 showed weak inhibition against T-L. In addition, compound **11** dramatically increased accumulation of ubiquitinated proteins in HL-60 cells in a dose and time dependent manner. Because ubiquitinated proteins are degraded by proteasome, dysfunctional proteasome will lead to high level intracelluar protein ubiquitination.[28,29]

How compound **11** inhibits the function of UPP system is still not fully certained. It might be directly binding the enzymatic cavities of proteasome, or disrupt the recycling of polyubiquitinated protein, or indirectly, by the generation of reactive oxygen species (ROS). Mounting evidence suggests oxidative stress could damage the function of UPP system and sequentially prompts apoptosis.[30,31] Rhabdastrellic acid-A has recently been reported to induce elevated caspase-3 expression in HL-60 cells.[32] Activation of caspase-3 is one of the downstream effects of ROS accumulation, and then mediates the apoptosis pathway.

Accordingly, rhabdastrellic acid-A as a small molecule with unusual structural pattern, is a new inhibitor and a modulator targeting the ubiquitin-proteasome system, and it is a promising lead compound for the treatment of cancer.

3. Experimental

3.1. General experimental procedures

Optical rotations were measured using a Pudolph Research Analytical Automatic Polarimeter; ^{1}H, ^{13}C, and 2D NMR spectra were recorded using a Bruker Avance-500 and Varian INOVA-500 NMR spectrometers, using TMS as an internal standard. The chemical

shifts were measured in δ (ppm) and coupling constants in hertz. HRESIMS data were measured using a LTQ-Obitrap Xl Thero Scientific and FT-MS_Bruker APEX IV (7.0T). Silica gel GF_{254} for TLC and H-silica gel (200–300 mesh) for CC were supplied by Qingdao Marine Chemical Company (Qingdao, China). Solvents and chemicals used for chromatography were purchased from Beijing Chemical Company (Beijing, China).

3.2. Animal material

The sponge *R. globostellata* Carter (Acorinidae) was collected off the coral reef of Hainan Island in the South China Sea, in June 2006. The species was identified by Nicole J. de Voogd (National Museum of Natural History). A voucher specimen has been deposited at the State Key Laboratory of Natural and Biomimetic Drugs, Peking University with the code HSF-10, and also deposited at the National Museum of Natural History.

3.3. Extraction and isolation

The freeze-dried sponge sample (4.7 kg) was homogenized and extracted with MeOH. The crude extract was partitioned between H_2O and CH_2Cl_2, and the CH_2Cl_2 layer was concentrated in vacuo to yield a fraction (6.0 g). This fraction was subsequently subjected to VLC, and eluted using a gradient system of petroleum ether (PE)–acetone to obtain ten fractions (FA-FJ). The fraction of FF (338 mg) was gel-filtered on a Sephadex LH-20 column (PE–CH_2Cl_2–MeOH, 5:5:1), and one of the collected fractions was separated upon C_{18} column chromatography (CC) eluting with MeOH–H_2O (8:1) to yield a mixture of **3** and **4** (2.2 mg). FG (540 mg) was separated by semi-preparative reversed-phase HPLC using MeOH–H_2O (45–65%) as a mobile phase to obtain **5** (6 mg), **7** (3.0 mg), **10** (4.6 mg), **8** (1.0 mg), **9** (0.8 mg), **11** (38.0 mg), **12** (28.0 mg), and **1** (14.0 mg). Using the same method as for FG, **6** (3.0 mg), **13** (3.8 mg), **14** (5.2 mg), and **2** (20.0 mg) were purified from FH (219 mg).

3.3.1. Globostelletin A (1)

Achroic oil; $[\alpha]_D$ −17.9 (*c* 0.7, MeOH); UV (MeOH) λ_{max} 244 nm; IR (KBr) ν_{max} 3379, 2965, 1781, 1707, 1463, 1385 cm^{-1}; ^1H and ^{13}C NMR data, see Tables 1 and 2; HRESIMS *m*/*z* 337.2010 $[M+H]^+$ (calcd for $C_{19}H_{29}O_5$, 337.2026).

3.3.2. Globostelletin B (2)

Light yellow oil; $[\alpha]_D^{20}$ 33.5 (*c* 1.0, MeOH); UV (MeOH) λ_{max} 249 nm; IR (KBr) ν_{max} 3433, 2958, 1705, 1635, 1384, 1026 cm^{-1}; ^1H and ^{13}C NMR data, see Tables 1 and 2; HRESIMS *m*/*z* 687.3867 $[2M+Na]^+$, (calcd for $(C_{20}H_{28}O_4)_2Na$, 687.3873).

3.3.3. Globostelletins C and D (3–4)

Light yellow oil; $[\alpha]_D^{20}$ −203.6 (*c* 0.11, MeOH); UV (MeOH) λ_{max} 307 nm; IR (KBr) ν_{max} 3416, 2959, 2931, 1703, 1383, 1111 cm^{-1}; ^1H and ^{13}C NMR data, see Tables 1 and 2; HRESIMS *m*/*z* 365.2087 $[M+Na]^+$ (calcd for $C_{22}H_{30}O_3Na$, 365.2094).

3.3.4. Globostelletin E (5)

Light yellow oil; $[\alpha]_D^{20}$ 12.3 (*c* 0.30, MeOH); UV (MeOH) λ_{max} 299 nm; IR (KBr) ν_{max} 3424, 2959, 1701, 1576, 1385, 1171, 1024 cm^{-1}; ^1H and ^{13}C NMR data, see Tables 1 and 2; HRESIMS *m*/*z* 359.2217 $[M+H]^+$ (calcd for $C_{22}H_{31}O_4$, 359.2224).

3.3.5. Globostelletin F (6)

Light yellow oil; $[\alpha]_D^{20}$ −6.2 (*c* 0.16, MeOH); UV (MeOH) λ_{max} 298 nm; IR (KBr) ν_{max} 3416, 2959, 1699, 1618, 1578, 1404 cm^{-1}; ^1H and ^{13}C NMR data, see Tables 1 and 2; HRESIMS *m*/*z* 359.2217 $[M+H]^+$ (calcd for $C_{22}H_{31}O_4$, 359.2215).

3.3.6. Globostelletin G (7)

Yellow oil; $[\alpha]_D^{20}$ −6.0 (*c* 0.25, MeOH); UV (MeOH) λ_{max} 340 nm; IR (KBr) ν_{max} 3421, 2928, 1696, 1383 cm^{-1}; ^1H and ^{13}C NMR data, see Tables 1 and 2; HRESIMS *m*/*z* 399.2530 $[M+H]^+$ (calcd for $C_{25}H_{35}O_4$, 399.2523).

3.3.7. Globostelletin H (8)

Yellow oil; $[\alpha]_D^{20}$ −50.0 (*c* 0.10, MeOH); UV (MeOH) λ_{max} 266, 367 nm; IR (KBr) ν_{max} 3416, 2962, 1619 cm^{-1}; ^1H and ^{13}C NMR data, see Tables 1 and 2; HRESIMS *m*/*z* 447.2506 $[M+Na]^+$ (calcd for $C_{27}H_{36}O_4Na$, 447.2516).

3.3.8. Globostelletin I (9)

Yellow oil; $[\alpha]_D^{20}$ −206.2 (*c* 0.08, MeOH); UV (MeOH) λ_{max} 269, 369 nm; IR (KBr) ν_{max} 3415, 2926, 1618, 1427, 1114 cm^{-1}; ^1H and ^{13}C NMR data, see Tables 1 and 2; HRESIMS *m*/*z* 425.2686 $[M+H]^+$ (calcd for $C_{27}H_{37}O_4$, 425.2675).

3.4. Cytotoxic assay

The cytotoxic activities of the isolated compounds were assessed using the MTT method. The cells were grown in DMEM media supplemented with 10% fetal bovine serum in a humidified atmosphere of 5% CO_2 and 95% air. The cells were incubated with varying concentrations of each compounds, and cell survival was detected at 37 °C by MTT method. The 5×10^3 cells in 100 μL of culture medium were grown in triplicate for 48 h in 96-well plates. MTT solution (15 μL) was then added to each well, and the samples were treated according to the manufacturer's protocol (Promega). The control values of cells were recorded by treatment with the DMSO alone.

3.5. Flow cytometry analysis of cell cycle

HL-60 cells (5×10^5) were inoculated in cell culture bottle by adding a certain dose of compound **11**, the cells were collected after a certain time. Each set of cells was washed with PBS, and was re-hanged in 0.3 mL PBS, which was fixed after rapid injection of 0.7 mL anhydrous ethanol (20 °C). Before analysis, ethanol is removed by washing with PBS. Cells were re-suspended in 0.5 mL PI dye solution (PBS containing 10 μg/mL PI and RNase A 50 μg/mL) at 37 °C in 30 min. Flow cytometry is used to detect cell cycle.

3.6. Cell apoptosis by flow cytometry

HL-60 cells (5×10^5) were inoculated in cell culture bottle to react with a certain dose of **11**. The cells were collected after centrifugation by 1000 rpm at 4 °C for 10 min to remove supernatant. Adding cold PBS (1.0 mL), the cell suspension was gently shocked. The above steps were repeated by twice. The cells were re-hanged in 200 μL binding buffer. Annexin V-FITC (10 μL) was added to mix gently for 30 min under dark at 4 °C. Then, binding buffer (300 μL) was added. Before test, PI (5 μL) was added, and the detection was performed within 1 h in the flow cytometry, and the data were read and analyzed by the application of Cellquest software.

3.7. Morphological observation of apoptosis

The process of sample preparation was in the same protocol as for the method of cell cycle. After detection by the flow cytometry, taking a small amount of cell suspension to drop on the glass slide, and covered with coverslip. Under a fluorescence microscope, the

morphological changes of cell apoptosis were observed, and were saved by camera photography.

3.8. Western blot analysis of protein expression in HL-60 cells

The HL-60 cells were collected after centrifugation. The cells (1×10^7) were washed by PBS, and the three detergent lysis solution (100 μL) (50 mM Tris–HCl (pH 7.5), 150 mM NaCl, 1% Nonidet P-40, 0.5% sodium deoxycholate, 0.1% sodium dodecyl sulfate SDS) was added at 4 °C in 30 min. Then, the sample buffer (fivefolds) was added to keep boiling for 5 min. dropping the solution (20 μL) over the 12% SDS–polyacrylamide gel electrophoresis, and transferred to a nitrocellulose membrane, 5% skimmed milk powder to cover at room temperature for 1.5 h. Afterward, first antibody (p21, 1:100 dilution) was added at 4 °C and kept overnight, and then separately reacted with the corresponding secondary antibody (mouse 1:4000) at room temperature for 1 h. Chemiluminescent substrate was colored, and B-actin was used as the control.

3.9. Assay of proteasome activity in vitro

The enzymatic activities of the proteasome were assayed using fluorogenic peptides: Suc-Leu-leu-Val-Tyr-AMC (Suc represents succinyl and AMC represents 7-amido-4methyicoumarin, obtained from SIGMA) for chymotryptic-like (ChT-L) and Boc-LRR-AMC for trypsin-like (T-L) activities. 1 μg of 20S proteasomes purified from human erythrocytes was incubated with various doses of 11 and 100 μM fluorogenic peptides in 100 μL of 20 mM Tris–HCl with pH 7.8 at 37 °C for 1 h. The fluorescence of released AMC was measured by a spectrofluorimeter (Fluostar OPTIMA, BMG Germany) at excitation/emission wavelengths of 380/440 nm. MG132 (1 μM), a known inhibitor of proteasome ChT-L activity and 0.1% DMSO were used as positive and solvent control. By comparison with the fluorescence of solvent control, the inhibitory effects were calculated using SigmaPlot software and a standard four parameter sigmoidal fit curve. Assays were performed in triplicate.

Acknowledgements

This work was supported by grants from NSFC (No. 30672607), the National Hi-Tech 863-Projects (2010DFA31610, 2007AA09Z448, 2007AA09Z435), and International Cooperation Projects of BMBF-MOST.

Supplementary data

Supplementary data associated with this article can be found, in the online version, at doi:10.1016/j.bmc.2010.05.029.

References and notes

1. Oku, N.; Matsunaga, S.; Wada, S.; Watabe, S.; Fusetani, N. *J. Nat. Prod.* **2000**, *63*, 205.
2. McCormick, J. L.; McKee, T. C.; Cardellina, J. H., II; Leid, M.; Boyd, M. R. *J. Nat. Prod.* **1996**, *59*, 1047.
3. Su, J. Y.; Meng, Y. H.; Zeng, L. M.; Fu, X.; Schmitz, F. *J. Nat. Prod.* **1994**, *57*, 1450.
4. Ryu, G.; Matsunaga, S.; Fusetani, N. *J. Nat. Prod.* **1996**, *59*, 512.
5. Tang, S.; Deng, Z.; Li, J.; Fu, H.; Pei, Y.; Zhang, S.; Lin, W. *Chin. Chem. Lett.* **2005**, *16*, 353.
6. Meragelman, K. M.; McKee, T. C.; Boyd, M. R. *J. Nat. Prod.* **2001**, *64*, 389.
7. Kobayashi, J.; Yuasa, K.; Kobayashi, T.; Sasaki, T.; Tsuda, M. *Tetrahedron* **1996**, *52*, 5745.
8. Tang, S.; Pei, Y.; Fu, H.; Deng, Z.; Li, J.; Proksch, P.; Lin, W. *Chem. Pharm. Bull.* **2006**, *54*, 4.
9. Ravi, B. N.; Wella, R. J. *Aust. J. Chem.* **1982**, *35*, 39.
10. Zhang, W.; Che, C. *J. Nat. Prod.* **2001**, *64*, 1489.
11. Tasdemir, D.; Mangalindan, G. C.; Concepcion, G. P.; Verbitski, S. M.; Rabindran, S. *J. Nat. Prod.* **2002**, *65*, 210.
12. Bourguet-Kondracki, M. L.; Longeon, A.; Debitus, C.; Guyot, M. *Tetrahedron Lett.* **2000**, *41*, 3087.
13. Fouad, M.; Edrada, R. A.; Ebel, R.; Wray, V.; Muller, W. E. G.; Lin, W. H.; Proksch, P. *J. Nat. Prod.* **2006**, *69*, 211.
14. Lv, F.; Deng, Z.; Li, J.; Fu, H.; van Soest, R. W.; Proksch, P.; Lin, W. *J. Nat. Prod.* **2004**, *67*, 2033.
15. Clement, J. A.; Li, M.; Hecht, S. M.; Kingston, D. G. I. *J. Nat. Prod.* **2006**, *69*, 373.
16. Lin, H.; Wang, Z.; Wu, J.; Shi, N.; Zhang, H.; Chen, W.; Susan, L. M. N.; Lin, A. *J. Nat. Prod.* **2007**, *70*, 1114.
17. Rao, Z.; Deng, S.; Wu, H.; Jiang, S. *J. Nat. Prod.* **1997**, *60*, 1163.
18. Liu, W.; Che, J. H. *Cancer Lett.* **2009**, *230*, 102.
19. Wei, S.; Li, M.; Tang, S.; Sun, W.; Xu, B.; Cui, J.; Lin, W. *Cancer Lett.* **2008**, *262*, 114.
20. Lodeiro, S.; Wilson, W. K.; Shan, H.; Matsuda, S. P. T. *Org. Lett.* **2006**, *8*, 439.
21. Domingo, V.; Arteaga, J. F.; Moral, J. F. Q.; Barrero, A. F. *Nat. Prod. Rep.* **2009**, *26*, 115.
22. Klaus, G.; Axel, G. *Tetrahedron* **1984**, *40*, 3235.
23. Eastman, A. *J. Cell. Biochem.* **2004**, *91*, 223.
24. Broemer, M.; Meier, P. *Trends Cell Biol.* **2009**, *19*, 130.
25. Monticone, M.; Biollo, E.; Fabiano, A. *Mol. Cancer Res.* **2009**, *7*, 1822.
26. Hussain, A. R.; Ahmed, M.; Ahmed, S. O. *Leuk. Lymphoma* **2009**, *50*, 1204.
27. Lu, G.; Punj, V.; Chaudhary, P. M. *Cancer Biol. Ther.* **2008**, *7*, 603.
28. Moore, B. S.; Eustáquio, A. S.; McGlinchey, R. P. *Curr. Opin. Chem. Biol.* **2008**, *12*, 434.
29. Kitagawa, K.; Kotake, Y. *Cancer Sci.* **2009**, *100*, 1374.
30. Davies, K. J. *Biochimie* **2001**, *83*, 301.
31. Halliwell, B. *Ann. N.Y. Acad. Sci.* **2002**, *962*, 182.
32. Guoa, J.; Zhoua, J.; Zhang, Y. *Cell Biol. Int.* **2008**, *32*, 48.